A Journal of the Gesellschaft Deutscher Chemiker

Angewandte International Edition

GDCh

Chemie

www.angewandte.org

Accepted Article

Title: Dynamically Monitoring Cell Viability in a Dual-Color Mode: Construction of an Aggregation/Monomer-Based Probe Capable of Reversible Mitochondria-Nucleus Migration

Authors: Minggang Tian, Jie Sun, Baoli Dong, and Weiying Lin

To be cited as: *Angew. Chem. Int. Ed.* 10.1002/anie.201811459
Angew. Chem. 10.1002/ange.201811459

Link to VoR: http://dx.doi.org/10.1002/anie.201811459
http://dx.doi.org/10.1002/ange.201811459

WILEY-VCH

10.1002/anie.201811459

WILEY-VCH

COMMUNICATION

Dynamically Monitoring Cell Viability in a Dual-Color Mode: Construction of an Aggregation/Monomer-Based Probe Capable of Reversible Mitochondria-Nucleus Migration

Minggang Tian, Jie Sun, Baoli Dong, and Weiying Lin*

Abstract: Mitochondria and nucleus play crucial roles during cell apoptosis process. In this work, a unique fluorescent probe capable of reversible migration between mitochondria and nucleus, as well as detection of cell viability in a dual-color mode is presented. The dual-color probe targets mitochondria in healthy cells, to form aggregates with deep-red emission. It migrates into nucleus and binds to DNA to form monomers with green fluorescence during apoptosis. Interestingly, the migration is reversible dependent on cell viability, which enables the dynamic visualization of apoptosis process. With the probe, mitochondria and nucleus can be visualized in dual colors during apoptosis, and the cell viability could be monitored by the emission color and localization of the probe.

Monitoring cell viability is a highly valuable task essential for the fundamental researches in biology, pathology, and medicine.[1,2] For instance, detecting the cell viability is necessary to evaluate the efficacy of drugs and the cytotoxicity of biological reagents, including antibiotics, drugs, nanoparticles, and fluorophores.[3-6] Meanwhile, changing of cell viability such as apoptosis and necrosis process under physiological conditions is indispensable to maintain the homeostasis of cell population, and to defend organisms in immune reactions.[7] Mitochondria and nucleus play significant roles in the change of cellular status, especially in apoptosis process.[8] According to the recent reports, the signalling process of apoptosis initiates from the changes in cell nucleus, including DNA damages and oncogene activation.[8] Meanwhile, the execution of cell apoptosis starts from mitochondria.[9,10] Mitochondria contain harmful proteins, reactive oxygen species, and some other toxic compounds, which are maintained inside mitochondria by their double membranes in healthy cells. During cell apoptosis, sudden change in the membrane permeability would occur and these toxic compounds could be released to the cytoplasm and trigger the apoptosis process.

To in-depth explore the relationship among mitochondria, nucleus, and cell viability, visualization of the two organelles and simultaneous detection of cell viability are greatly helpful. Up to now, scanning electron microscope, transmission electron microscope, colorimetric analysis, optical microscope, and many other tools have been widely used to study mitochondria, nucleus, and cell viability.[11-15] Compared with these techniques, fluorescence imaging methods assisted with proper fluorescent probes have received considerable interest in recent years, owing to the unique advantages including capability of *in situ* and real-time visualization in live cells, low damage to biosamples, and permission of dynamically analyzing live samples.[16,17] For example, Kim *et al.* have designed and synthesized a mitochondria immobilized fluorescent probe to investigate the mitochondrial dynamics during mitophagy processes.[18] Teulade-Fichou and co-workers have developed two-photon fluorescent probes for the imaging of cell nucleus.[19] Eliseeva *et al.* have presented a near infrared fluorescent probe for the discrimination of dead cells.[20]

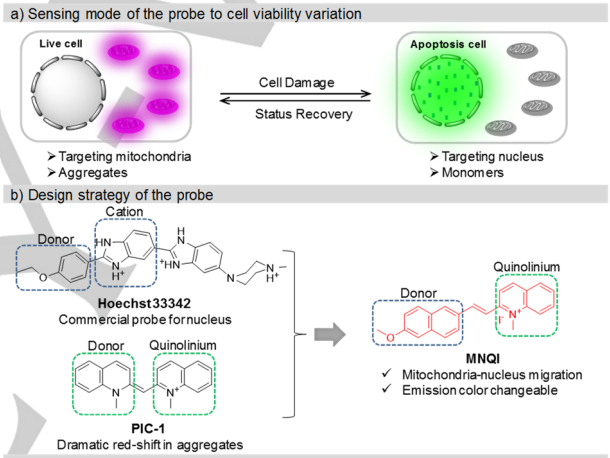

Scheme 1. (a) The sensing mode of the mitochondria-nucleus migration probe for detecting cell viability. (b) The design strategy of **MNQI**.

Recently, Kawamata's group, Yu's group, and Tian's group have developed fluorescent probes which target mitochondria in healthy cells and gradually migrate into nucleus/nucleolus during apoptosis.[21-23] The fluorescence wavelengths of those probes remain unchanged in mitochondria and nucleus. However, these intensity-based probes have some limitations, such as the interferences from inhomogeneous staining of probes and fluctuation of excitation intensity.[16] To avoid these limitations, it is essential to discriminatively visualize mitochondria and nucleus in dual emission colors. Unfortunately, fluorescent probes capable of visualization of mitochondria and nucleus in dual emission channels, and simultaneously enabling the detection of cell viability have not been reported yet, which is an extremely challenging task.

In this work, we have designed and synthesized a fluorescent probe **MNQI** based on aggregation/monomer mechanism, for the visualization of the two organelles in dual channels, and the detection of cell viability. In Scheme 1, **MNQI** was constructed with a weak electronic donor and a cationic quinolinium group. It was a hydrophobic cation in nature which could be enriched in mitochondria with high negative MMP in healthy cells. Moreover, due to its structural similarity to PIC[24] and high concentration in

Dr. M. Tian, J. Sun, Dr. B. Dong, Prof. W. Lin
Institute of Fluorescent Probes for Biological Imaging, School of Chemistry and Chemical Engineering, School of Materials Science and Engineering, University of Jinan, Jinan, Shandong 250022, People's Republic of China
E-mail: weiyinglin2013@163.com
Supporting information for this article is given via a link at the end of the document.

10.1002/anie.201811459

mitochondria, **MNQI** forms aggregates with deep-red (DR) emission in healthy cells.

The electronic structure of **MNQI** resembles Hoechst, with a weak electronic donor and a positively charged group. This similarity endows **MNQI** high affinity to DNA. Therefore, with the decrease of MMP in unhealthy status, the probe could be released from mitochondrial and migrate into nucleus to form monomers in DNA with green fluorescence. The migration of **MNQI** between mitochondria and nucleus is dependent on MMP and reversible. Consequently, cell viability could be evaluated by the localization and intracellular emission color of **MNQI**.

The optical properties of the probe were initially investigated. According to the molecular design, a prerequisite is that the probe displays different emission wavelengths in the aggregation and monomer states. Consequently, the absorption and fluorescence spectra of **MNQI** in different organic solvents were acquired to check the optical properties of its monomers. Simultaneously, the emission spectra in buffer solutions and the solid state were also obtained to explore the property of its aggregates. As shown in Figure 1a and S1, **MNQI** displays strong absorbance in 350-500 nm and emission peaked around 570 nm in organic solvents. The probe shows blue-shifted absorption and weak emission peaked at 570 nm in buffer solutions, indicating that it forms H-aggregates in aqueous conditions. Fortunately, **MNQI** exhibits strong fluorescence peaked at 690 nm in solid state. Thus, **MNQI** shows emission peaked at 570 nm and 690 nm in organic solvents and solid states, respectively, demonstrating that the probe could give dual emission colors in aggregation and monomer states.

To testify the mechanism of the red shift in aggregation state of **MNQI**, its crystal has been prepared and analysed to investigate the packing mode in solid state. In Figure 1b and 1c, the molecules of **MNQI** are anti-parallelly stacked and form dimers in the crystalline state, due to intermolecular electrostatic interactions. The short intermolecular stacking distances of the dimer are 3.364 Å, 3.340 Å, and 3.312 Å, indicating strong intermolecular interactions inside the dimer. Moreover, the short stacking distances between dimers are 3.374 Å and 3.390 Å, demonstrating that interactions also exist between the dimers. Consequently, the red shift in solid state should be attributed to the intermolecular π-π interactions induced by the short contact between the molecules.

In order to target cell nucleus, the probe should exhibit high affinity to DNA, since the majority of cellular DNA exists in the nucleus. Therefore, the DNA titration experiments have been performed with **MNQI**. In Figure S2, **MNQI** displays rather weak fluorescence in buffer solution, owing to the formation of H-aggregates. With the addition of DNA, the fluorescence gradually enhanced to 6-fold, because of the formation of monomers when binding to DNA. The binding coefficient (k) is calculated as 4.1 × 10^6 M^{-1}, following the Scatchard equation (Figure S2), indicating its high affinity to DNA that is slightly lower than Hoechst 33342 (2 × 10^7 M^{-1}),[25] a commercial probe for DNA.

To explore the binding mechanism of **MNQI** to DNA in molecular level, molecular docking calculations based on the crystal structure of **MNQI** and DNA have been performed using AutoDock 4.2 software[26]. In Figure 1a, **MNQI** bound to the minor grooves of DNA, and the binding energy was calculated to be -9.45 kcal/mol. The binding of Hoechst 33342 to DNA has been also calculated for comparison. In Figure S3, Hoechst 33342 also bound to the minor grooves of DNA, and the binding energy was calculated as -12.0 kcal/mol. These results indicate the desirable affinity to DNA of **MNQI**, which is comparable to Hoechst 33342. The planar structure and electronic structure of **MNQI** should be responsible for its high affinity to DNA.

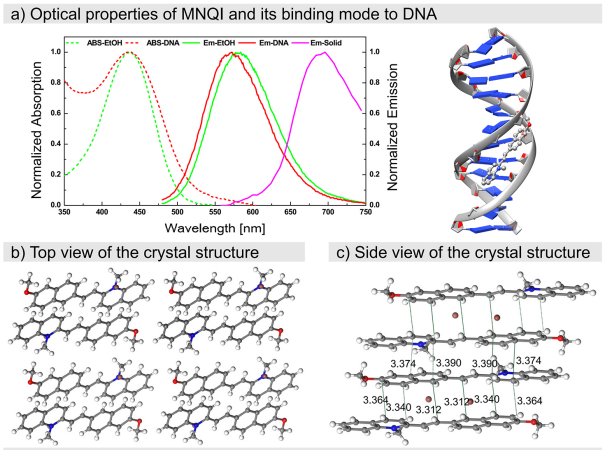

Figure 1. (a) The absorption and fluorescence spectra of 10 μM **MNQI** in ethanol, DNA solutions, and solid states, and the binding mode to DNA. λ_{ex} = 488 nm. The top view (b) and side view (c) of the crystal structure of **MNQI**.

In consideration of the strong affinity to DNA and positively charged nature of **MNQI**, the probe ought to target nucleus and mitochondria in cells. Before cell imaging applications, the cytotoxicity of **MNQI** to live cells has been initially testified using MTT assay. In Figure S4, treatment with 1-15 μM **MNQI** for 24 h brings little toxicity to live cells, and cell viability is above 90 %. Thus, the cytotoxicity of 4 μM **MNQI** could be ignored with the incubation time in 1 h.

Live cells were stained with the probe and imaged in dual channels to check the localization of the probe. In Figure S5a, **MNQI** distributed in cytoplasm of live cells and gave strong fluorescent signals in the DR channel, while displayed weak emission in the green channel. Meanwhile, the DR fluorescence appeared as filament morphologies in cytoplasm, indicating the staining of mitochondria in live cells. The in situ fluorescence spectra have also been obtained using the spectral imaging function of the confocal microscope. In Figure S6, intracellular emission was peaked around 670 nm, resembling that of solid **MNQI**, and proving the formation of aggregates like the solid state.

Furthermore, fixed HeLa cells have also been stained with **MNQI** and imaged. In Figure S5a, **MNQI** stained the nucleus in fixed cells and displayed strong fluorescence only in the green channel. The in situ fluorescence spectra of **MNQI** in dead cells have also been acquired, and in Figure S6 the emission was peaked around 580 nm, similar with that in organic solvents and DNA solutions. These results proved that **MNQI** stained nucleus in fixed cells and presented in monomer state.

To accurately confirm the localization of **MNQI** in live and fixed cells, co-localization experiments with MTDR and Hoechst 33342, the commercialized probes for mitochondria and nucleus, have been performed. In Figure 2, the fluorescent signals from **MNQI** in live cells overlap well with that of MTDR, and the co-localization coefficient is up to 0.90, indicating that **MNQI** actually stained mitochondria in live cells. Moreover, the green emission from

10.1002/anie.201811459

MNQI in dead cells shows large overlap to the blue signals from Hoechst 33342, with the co-localization coefficient of 0.91, demonstrating that **MNQI** selectively stained nucleus in fixed cells. Therefore, **MNQI** can discriminate live and fixed cells through the localization and emission color of intracellular fluorescent signals.

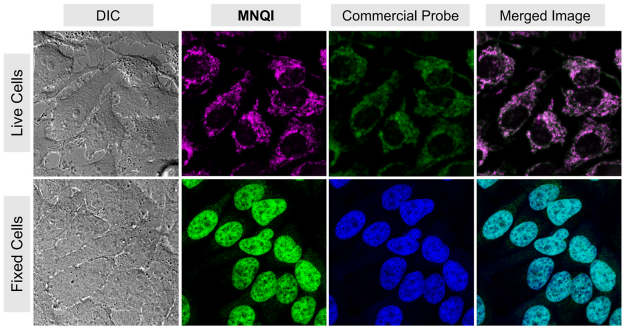

Figure 2. The images of live and fixed HeLa cells co-stained with 4 μM **MNQI** and commercial probes (200 nM MTDR for live cells, 2 μM Hoechst 33342 for fixed cells) for 60 min. **MNQI** in live cells: λ_{ex} = 488 nm, λ_{em} = 570-620 nm; MTDR: λ_{ex} = 647 nm, λ_{em} = 663-738 nm; **MNQI** in dead cells: λ_{ex} = 488 nm, λ_{em} = 500-550 nm; Hoechst 33342: λ_{ex} = 405 nm, λ_{em} = 425-475 nm. Bar = 10 μm.

MNQI targets mitochondria and nucleus in live and fixed cells, respectively. We speculate that the distribution of **MNQI** is determined by the MMP levels. In live cells with high MMP, **MNQI** mainly exists in mitochondria due to the electrophoresis effect. In dead cells with almost no MMP, **MNQI** targets nucleus due to the affinity to DNA. To prove the speculation, healthy HeLa cells were prestained with **MNQI**, and then treated with CCCP, a regent that can decrease MMP rapidly. In Figure 3a and Movie S1, **MNQI** initially stained mitochondria with DR emission in healthy cells. With the addition of CCCP and decrease of MMP levels, **MNQI** was released from mitochondria and migrated to the nucleus with green emission. Subsequently, MMP levels could actually influence the targets of **MNQI**. CCCP was afterwards removed and MMP levels could be recovered. In Figure 3b, after the removal of CCCP, the green emission in nucleus gradually disappeared, indicating that **MNQI** migrated back into mitochondria. This procedure can be semi-quantified by the ratio of green to DR signals shown in Figure 3c. These results indicate that **MNQI** could reversibly detect the changes of MMP levels from both the localization and the emission color. Considering that MMP levels could directly reflect the cell viability, **MNQI** is potential to report the cell viability reversibly.

Excessive amount of hydrogen peroxide could inhibit the oxidation respiratory chain and induce cell damage.[27] To verify the ability of **MNQI** in visualization of cell viability, healthy cells pre-incubated with **MNQI** were treated with hydrogen peroxide (Figure S7 and Movie S2). In Figure S7a, healthy cells displayed strong DR emission in mitochondria and almost no emission in nucleus. After the addition of hydrogen peroxide, cell viability was decreased, and green emission in the nucleus steadily enhanced, indicating the migration of **MNQI** from mitochondria to nucleus. This process could be also monitored by the signal ratio of green channels to DR ones, as plotted in Figure S7c. These results confirmed that **MNQI** could serve a valid tool for visualizing the decline of cell viability through both the localization and emission color.

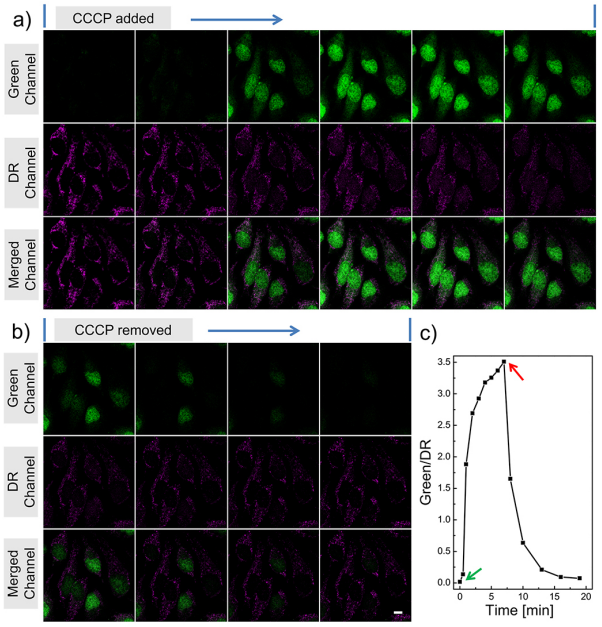

Figure 3. Fluorescence images of HeLa cells pre-stained with 4 μM **MNQI** for 60 min, (a) treated with 20 μM CCCP for 0-7 min, and then (b) CCCP was washed away and incubated with culture medium for another 1-12 min. (c) The time-dependent intensity ratio of green channel to DR channel in (a) and (b). λ_{ex} = 488 nm; green channel: λ_{em} = 500-550 nm; DR channel: λ_{em} = 663-738 nm. Bar = 10 μm.

L-Ascorbic acid (VC) is a significant antioxidant resistant to damage by ROS. Consequently, we conceived that VC may recover the status of cells pretreated with hydrogen peroxide for a short period of time. In Figure S7b, after the treatment for 15 min, hydrogen peroxide was removed and VC was added. Obviously, the green emission in nucleus faded off, indicating the migration of **MNQI** back into the mitochondria and the recovery of cell viability. The process could also be monitored (Figure S7c) by means of the intensity ratio between the two emission channels. Therefore, **MNQI** can detect the reversible change of cell viability.

Rotenone is a toxicant that has been used as a broad-spectrum pesticide, which can efficiently induce cell apoptosis.[28] Recent studies revealed that rotenone worked by interfering with the electron transport chain in mitochondria, and caused the excess production of ROS.[28] To discover the potential application of **MNQI** to discriminate apoptosis cells, live HeLa cells was pretreated with rotenone for 24 h and then stained with the probe (Figure 4a). Live cells in the control group untreated with rotenone displayed intense DR emission in mitochondria and no fluorescence in the nucleus. In comparison, cells treated with rotenone displayed strong emission in green channel and weakened fluorescence in DR channel, indicating cell apoptosis and decreased viability. In Figure 7b, the ratio of green to DR channel exhibited dramatic increase upon the treatment of rotenone, also demonstrating the cell apoptosis.

Since rotenone induces cell apoptosis by promoting the generation of elevated levels of ROS, VC may be able to relieve the toxicity owing to its anti-oxidative characteristics. Consequently, VC was added to cells pretreated with rotenone for 6 h, and then the cells were further cultured for another 18 h. In Figure 5a, VC-treated cells display obviously weakened green emission and enhanced DR fluorescence, compared with those

10.1002/anie.201811459

solely incubated with rotenone. This could also be clearly observed via the signal ratio of green to red channel (Figure 5b). Accordingly, **MNQI** could detect the apoptosis process induced by rotenone, via the change of localization and emission color. The effect of VC to relieve rotenone toxicity could also be visualized.

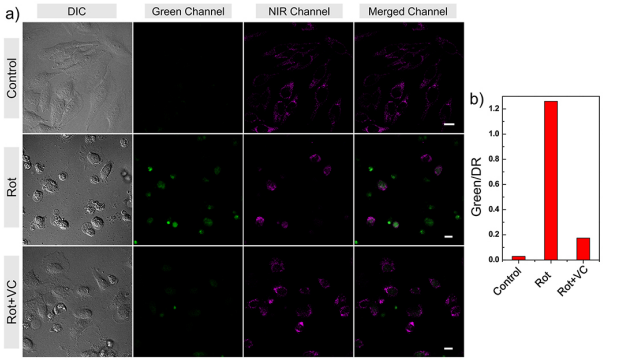

Figure 4. (a) DIC and fluorescent images of HeLa cells stained with 4 μM **MNQI** for 60 min after the incubation with different regents, and (b) the corresponding intensity ratio of green channel to DR channel. Control group: HeLa cells were treated with DMSO for 24 h; "Rot" group: HeLa cells were incubated with 5 μM rotenone for 24 h; "Rot+VC" group: HeLa cells were treated with 5 μM rotenone for 6 h, then 100 μM VC was added, and the cells were incubated for another 18 h. λ_{ex} = 488 nm; green channel: λ_{em} = 500-550 nm; DR channel: λ_{em} = 663-738 nm. Bar = 10 μm.

In conclusion, we have designed and synthesized an aggregation/monomer-based fluorescent probe, **MNQI**, capable of reversible migration between nucleus and mitochondria, and visualization of dynamic changes in cell viability in a dual-color mode. The cationic probe could stain mitochondria in healthy cells, and form aggregates with DR-emissive properties. Along with the decrease of cell viability, the novel probe could be released from mitochondria and migrate into nucleus to emit green fluorescence in monomer status. Meanwhile, with the recovery of the cell viability, **MNQI** can reversibly move back to the mitochondria with DR emission. Using this unique probe, the cell viability could be dynamically and accurately visualized through the intracellular localization and emission color. Particularly, the reversible changes of cell viability have been successfully observed with the probe. The cell apoptosis caused by toxic rotenone has been detected using **MNQI**, and the inhibition effect of VC to rotenone caused apoptosis was verified. We believe that **MNQI** can serve as a powerful tool to investigate the internal relationship among apoptosis, nucleus, and mitochondria, and promote the fundamental researches in biology, pathology, and medicine.

Acknowledgements

This work was financially supported by NSFC (21472067, 21672083, 21877048, 21804052), Taishan Scholar Foundation (TS201511041), NSF of Shandong Province (ZR2018BB058), and the startup fund of University of Jinan (309-10004, 160100331).

Conflict of interest

The authors declare no conflict of interest.

Keywords: fluorescent probe • cell viability • mitochondria • nucleus • dual-color

Reference

[1] O. Kepp, L. Galluzzi, M. Lipinski, J. Yuan, G. Kroemer, *Nat. Rev. Drug Discov.* **2011**, *10*, 221-237.
[2] V. Vichai, K. Kirtikara, *Nat. Protoc.* **2006**, *1*, 1112-1116.
[3] V. M. Steffes, M. M. Murali, Y. Park, B. J. Fletcher, K. K. Ewert, C. R. Safinya, *Biomaterials* **2017**, *145*, 242-255.
[4] R. Alford, H. M. Simpson, J. Duberman, G. C. Hill, M. Ogawa, C. Regino, H. Kobayashi, P. L. Choyke, *Mol. Imaging* **2009**, *8*, 341-354.
[5] N. Lewinski, V. Colvin, R. Drezek, *Small* **2008**, *4*, 26-49.
[6] F. Valeriote, P. L. Van, *Cancer Res.* **1975**, *35*, 2619.
[7] S. Elmore, *Toxicol. Pathol.* **2007**, *35*, 495-516.
[8] E. A. Prokhorova, A. V. Zamaraev, G. S. Kopeina, B. Zhivotovsky, I. N. Lavrik, *Cell. Mol. Life Sci.* **2015**, *72*, 4593-4612.
[9] S. W. Tait, D. R. Green, *Nat. Rev. Mol. Cell Biol.* **2010**, *11*, 621-632.
[10] N. Zamzami, G. Kroemer, *Nat. Rev. Mol. Cell Biol.* **2001**, *2*, 67-71.
[11] G. Repetto, A. del Peso, J. L. Zurita, *Nat. Protoc.* **2008**, *3*, 1125-1131.
[12] M. L. Joiner, O. M. Koval, J. Li, B. J. He, C. Allamargot, Z. Gao, E. D. Luczak, D. D. Hall, B. D. Fink, B. Chen, J. Yang, S. A. Moore, T. D. Scholz, S. Strack, P. J. Mohler, W. I. Sivitz, L. S. Song, M. E. Anderson, *Nature* **2012**, *491*, 269-273.
[13] T. D. Allen, S. A. Rutherford, S. Murray, F. Gardiner, E. Kiseleva, M. W. Goldberg, S. P. Drummond, *Nat. Protoc.* **2007**, *2*, 1180-1184.
[14] B. Glancy, L. M. Hartnell, D. Malide, Z. X. Yu, C. A. Combs, P. S. Connelly, S. Subramaniam, R. S. Balaban, *Nature* **2015**, *523*, 617-620.
[15] H. Tominaga, M. Ishiyama, F. Ohseto, K. Sasamoto, T. Hamamoto, K. Suzuki, M. Watanabe, *Anal. Commun.* **1999**, *36*, 47-50.
[16] L. Yuan, W. Lin, K. Zheng, S. Zhu, *Acc. Chem. Res.* **2012**, *46*, 1462-1473.
[17] R. Wayne, *Chapter 11 - Fluorescence Microscopy*, Elsevier Inc., **2014**.
[18] M. H. Lee, N. Park, C. Yi, J. H. Han, J. H. Hong, K. P. Kim, D. H. Kang, J. L. Sessler, C. Kang, J. S. Kim, *J. Am. Chem. Soc.* **2014**, *136*, 14136-14142.
[19] B. Dumat, G. Bordeau, E. Faurel-Paul, F. Mahuteau-Betzer, N. Saettel, G. Metge, C. Fiorini-Debuisschert, F. Charra, M. P. Teulade-Fichou, *J. Am. Chem. Soc.* **2013**, *135*, 12697-12706.
[20] I. Martinic, S. V. Eliseeva, T. N. Nguyen, V. L. Pecoraro, S. Petoud, *J. Am. Chem. Soc.* **2017**, *139*, 8388-8391.
[21] H. Moritomo, K. Yamada, Y. Kojima, Y. Suzuki, S. Tani, H. Kinoshita, A. Sasaki, S. Mikuni, M. Kinjo, J. Kawamata, *Cell Struct. Funct.* **2014**, *39*, 125-133.
[22] X. Li, M. Tian, G. Zhang, R. Zhang, R. Feng, L. Guo, X. Yu, N. Zhao, X. He, *Anal. Chem.* **2017**, *89*, 3335-3344.
[23] D. Liu, M. Zhang, W. Du, L. Hu, F. Li, X. Tian, A. Wang, Q. Zhang, Z. Zhang, J. Wu, Y. Tian, *Inorg. Chem.* **2018**, *57*, 7676-7683.
[24] N. J. Hestand, F. C. Spano, *Chem. Rev.* **2018**, *118*, 7069-7163.
[25] R. S. Harapanhalli, L. W. McLaughlin, R. W. Howell, D. V. Rao, S. J. Adelstein, A. I. Kassis, *J. Med. Chem.* **1996**, *39*, 4804-4809.
[26] G. M. Morris, R. Huey, W. Lindstrom, M. F. Sanner, R. K. Belew, D. S. Goodsell, A. J. Olson, *J. Comput. Chem.* **2009**, *30*, 2785-2791.
[27] M. Das, S. B. Mukherjee, C. Shaha, *J. Cell Sci.* **2001**, *114*, 2461-2469.
[28] N. Li, K. Ragheb, G. Lawler, J. Sturgis, B. Rajwa, J. A. Melendez, J. P. Robinson, *J. Biol. Chem.* **2003**, *278*, 8516-8525.

10.1002/anie.201811459

WILEY-VCH

Entry for the Table of Contents (Please choose one layout)

COMMUNICATION

Visualizing cell viability in dual-color mode: A fluorescent probe capable of reversible migration between mitochondria and nucleus dependent on cell viability and labelling the two organelles in dual colors has been developed. With the probe, mitochondria and nucleus can be visualized in dual emission channels, and cell viability could be evaluated by intracellular emission color and probe localization.

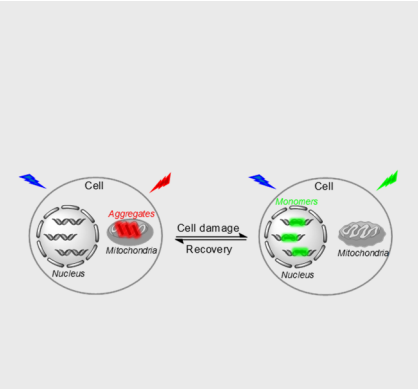

*Minggang Tian, Jie Sun, Baoli Dong, and Weiying Lin**

Page No. – Page No.

Dynamically Monitoring Cell Viability in a Dual-Color Mode: Construction of an Aggregation/Monomer-Based Fluorescent Probe Capable of Reversible Mitochondria-Nucleus Migration